On the implications of nitromethane - NO_x chemistry interactions for combustion processes

Krishna Prasad Shrestha[1, *], Lars Seidel[2], Thomas Zeuch[3], Gladys Moréac[4, 5], Philippe Dagaut[5], and Fabian Mauss[1]

1. Thermodynamics and Thermal Process Engineering, Brandenburg University of Technology, Siemens-Halske-Ring 8, 03046 Cottbus, Germany
2. LOGE Deutschland GmbH, Burger Chaussee 25, 03044 Cottbus, Germany
3. Institut für Physikalische Chemie, Georg-August-Universität Göttingen, Göttingen, Germany
4. RENAULT SAS, 78084 Guyancourt, France
5. ICARE, Centre National de la Recherche Scientifique (CNRS-INSIS), Orléans, France

***Corresponding author:** Krishna Prasad Shrestha

e-mail: shrestha@b-tu.de

Abstract

In this work, we report a detailed investigation of the CH_3NO_2 chemistry effect on fuel-NO interactions for the fuels methane and *n*-heptane using a recently developed and extensively validated $H_2/O_2/CO/NO_x/NH_3/CH_3NO_2$ baseline chemistry. In general, the model predictions show good agreement with temperature profiles of major and intermediate species in jet-stirred reactor experiments and they capture the subtle effect of NO addition. For both fuels, the CH_3NO_2 kinetics retard the system reactivity in the low temperature range by delaying the production of key radicals like OH and HO_2. This explains the retarding effect of NO for *n*-heptane low temperature ignition and the overprediction of reactivity enhancement by NO in earlier studies on methane combustion. For methane, the recently explored roaming mediated dissociation channel of CH_3NO_2 to CH_3O + NO is a major reaction pathway for CH_3NO_2 consumption. Our analysis suggests that at higher pressure, relevant to engine conditions, the two key intermediate species HONO and CH_3NO_2 feature strongly increased concentrations during *n*-heptane combustion and they may be detectable under such conditions in combustion experiments of this fuel-NO_x system. The results of this work call for detailed future investigations of the CH_3NO_2 chemistry effect in the context of exhaust gas recirculation, also with regard to the suppression of engine knock.

Keywords: Nitromethane, NO_x, fuel-NO_x, kinetic modeling, EGR

1. Introduction

Unraveling the molecular mechanisms of complex reaction sequences is a central goal of chemical research. A valid reaction mechanism gives predictive power to kinetic simulations with potentially drastic implications for addressing environmental issues and industrial applications. The understanding of the creation and the subsequent containment of the hole in the ozone layer is perhaps the best-known example in this context [1]. Complex gas-phase reaction systems govern the oxidation of hydrocarbons in the atmosphere and during combustion [2]. Missing or unreliable kinetic data on single chemical steps can alter the mechanistic understanding of important chemical phenomena like new particle formation in the troposphere [3] or pollutant formation in flames [4]. The severe underestimation of the reaction rate of Criegee intermediates (CI) with SO_2 [3] and wrong product assignments for the $CH_3 + O$ [5] and $CH + N_2$ [4,6] reactions in hydrocarbon flames are prominent examples of the last decades that motivate efforts in kinetic research up to now [2].

In combustion chemistry, the understanding of NO_x formation and measures for NO_x reduction in internal combustion engines are important fields of current research [7,8]. The conflict of objectives in the desired reduction of both NO_x and CO_2 emissions has recently come to a political crisis in the context of European clean air legislation and the growing establishment of "no drive zones" even for relatively new Diesel cars. One widely applied measure for reducing NO_x in Internal combustion (IC) engines is exhaust gas recirculation (EGR) which introduces preformed NO to the ignition process promoting ignition and decreasing temperature and NO_x emissions [9]. The enhanced auto-ignition effect has been attributed to a mutual sensitization of fuel and NO oxidation [10,11]. However, the details of the underlying mechanisms and the effect of fuel molecules larger than methane have not been rigorously explored so far. In the case of n-heptane e.g., NO addition reduces ignitability in the low temperature range [12]. In general, the chemistry of N-atom carrying radicals has gained again attention in recent years, e.g. with regard to the role of NCN in NO formation [6] and ammonia as a hydrogen carrier or storage compound [13]. This situation calls for developing comprehensive kinetic models that cover the now enlarged range of relevant fuels and combustion conditions. To this end, we have, in a first step, compiled and extensively validated an $H_2/O_2/CO/NO_x$ mechanism, successfully extended to simulate the oxidation of ammonia. The simulations have elucidated the strong influence of the HO_2 radical concentrations on reducing or oxidizing NO_x conditions [14]. In our subsequent study, we extended the model [14] and introduced C_1-C_2 chemistry covering hydrocarbons as well as alcohols (C_1-C_2) as fuel [15]. In our most recent experimental and modeling work [16], we extended our nitrogen chemistry introducing nitromethane as a fuel. Similar to our previous works [14,15], the model was validated for a broad range of experimental conditions and setups (speciation in jet-stirred and flow reactors and premixed flames, laminar flame speeds and ignition timing). The model development approach is hierarchically in nature. In the present

study, this enabled a comprehensive re-examination of the ignition timing during methane and, as a model system for exhaust gas recirculation in engines, *n*-heptane oxidation with premixed NO_x. Very recently, significant progress has been made on the experimental side with regard to the effect of NO addition. In 2018, Battin-Leclerc and co-workers [17] conducted an experimental and modeling study of methane oxidation in the presence of NO_x in a jet-stirred reactor at 106.7 kPa. They tried to quantify the species HONO and CH_3NO_2 in their experiment but were not successful in that work, concluding that these species were below the estimated detection limit of 3 and 5 ppm respectively. However, in 2019 Battin-Leclerc and co-workers succeeded in measuring HONO quantitatively using continuous-wave Cavity Ring-Down Spectroscopy (cw-CRDS) in a follow-up study [18] on *n*-pentane oxidation in the presence of NO (500 ppm) in a jet-stirred reactor at 106.7 kPa under stoichiometric conditions. The determined peak concentration of HONO was 256 ppm (± 24 ppm); however, the detection of CH_3NO_2 was not reported. This is clearly an important step in improving our understanding of the specific low-temperature oxidation chemistry of fuel – NO_x systems and the question arises if there are conditions under which CH_3NO_2 can be detected. In this study, we make use of the recent progress in characterizing chemical NO_x/CH_3NO_2 fuel interactions for a detailed kinetic modelling study of the mechanism of the exhaust gas recirculation effect, augmenting the experimental target range by jet stirred reactor experiments on *n*-heptane oxidation in the presence of NO. The ensuing analysis illustrates the crucial role of nitromethane chemistry for this important industrial application and identifies experimental conditions under which an *in-situ* detection of CH_3NO_2 may be achieved.

2. Kinetic Model

The complete nitromethane/NO_x kinetic model used in this work comes from our recently published work Shrestha et. al. [16] which was built hierarchically and validated for a wide range of experimental conditions (speciation in a jet-stirred and flow reactor, speciation in premixed flames, laminar flame speeds and ignition delay times). In this recent study [16] the roaming isomerization path of nitromethane was introduced, where nitromethane can isomerize to methyl nitrate (CH_3ONO) finally dissociating to CH_3O+NO ($CH_3NO_2 \rightarrow CH_3ONO \rightarrow CH_3O$+NO). The importance of this path was not shown in previously published literature models. A detailed description of this pathway can be found in our recent work [16].

In the present work, two fuels are investigated namely methane (CH_4) and n-heptane (*n*-C_7H_{16}). For methane oxidation, our recently published kinetic model [16] is used which was validated broadly (speciation in a jet-stirred and flow reactor, speciation in premixed flames, laminar flame speeds and ignition delay times) for H_2, NH_3, C_1-C_2 fuels including NO_x chemistry which can be found in our previous study Shrestha et. al. [14,15]. The *n*-heptane kinetic scheme used in this study is taken from a previous experimental and modeling study (Seidel et. al. [19]) with a focus on *n*-heptane flame chemistry. The *n*-heptane mechanism was also validated in a multi setup experiment using literature data (see [19] for *n*-heptane model validation).

To describe the oxidation of *n*-heptane/NO_x blends and the impact of nitromethane kinetics, the complete nitrogen chemistry (which also includes nitromethane) from [16] is coupled with the *n*-heptane kinetic scheme from Seidel et al. [19]. The thermochemistry data and transport properties of the species are also taken from [16] and [19]. The complete n-heptane/nitrogen chemistry model consists of 402 species and 2543 reversible reactions which is provided in the supplementary material (SM).

2.1 Brief overview of nitromethane decomposition

Since this study demonstrates the importance of the CH_3NO_2 chemistry during fuel/NO_x interaction, before moving ahead we will discuss briefly on CH_3NO_2 decomposition chemistry.

During the fuel oxidation in presence of NO_x nitromethane is mainly formed through the recombination of CH_3 and NO_2 [15,20]. Nitromethane itself as a fuel can undergo thermal decomposition to form CH_3 and NO_2 [16]. However, several recent studies [21–25] on the thermal decomposition of CH_3NO_2 suggest that CH_3NO_2 not only thermally dissociates to CH_3+NO_2 , but can also isomerize to methyl nitrate (CH_3ONO) *via* a roaming type transition state finally dissociating to CH_3O+NO. Zhu and Lin [21] studied the CH_3NO_2 decomposition theoretically and suggested that the channel to CH_3O+NO could be detected in experiments. The theoretical analysis by Annesley et al. [24] suggests that at pressures above 2 Torr the product distribution undergoes a sharp transition from the roaming dominated ($CH_3ONO \rightarrow CH_3O$+NO) to the bond-fission dominated (CH_3+NO_2) channel. Hence the bond fission channel is dominating for combustion environments featuring significantly higher pressures in agreement with the studies mentioned above. Furthermore, this finding is supported by the later study of Matsugi and Shiina [25] who proposed branching ratios of 0.97 and 0.03 in favor of the C-N bond fission channel (CH_3+NO_2). Despite its low branching ratio of the CH_3O+NO channel, it is clearly recommended to take into account the roaming type channel in kinetic modeling studies [26].

Nitromethane can also undergo decomposition through secondary reaction channels: it can react with H atoms to yield CH_3+HNO_2, CH_3NO+OH, and CH_2NO_2+H_2. CH_3NO_2 can also react with OH radicals to form CH_2NO_2+H_2O or CH_3OH+NO_2. Furthermore, CH_3NO_2 can undergo H abstraction reacting with radicals such as O, HO_2, O_2, NO_2, CH_2-3, CH_2-1, CH_3, CH_3O, and C_2H_5 mainly forming CH_2NO_2 and the related products. The detailed discussion on the adopted rate parameters for the decomposition channels of nitromethane can be found in our previous work [15,16].

3. Results and Discussion

In all the figures shown below the solid lines represent the predictions without nitromethane chemistry and the dashed lines represent those with nitromethane chemistry unless stated differently. The symbols in the figures are the experimental data from our previous work [10–12]. All the simulations are performed with LOGEresearch v1.10 [27].

3.1. Effect of CH_3NO_2 kinetics on CH_4 oxidation in the presence of NO

In Fig. 1 the results of an experiment under fuel-lean conditions (φ=0.5) for 2.5% CH_4 and 1 % O_2 in nitrogen are shown for neat CH_4 and with 200 ppm NO added [10]. These jet-stirred reactor experiments are simulated using a perfectly stirred reactor model. In the upper panel (Fig. 1a) the steady-state concentrations of the methane, CO, and CO_2 are plotted as a function of reactor temperature (symbols) and compared to simulations with two versions of the here presented model, one with (dashed line) and one without (solid line) the CH_3NO_2 sub-mechanism. The comparison reveals that the model without CH_3NO_2 chemistry is incomplete and unable to predict the onset temperature for fuel conversion and the breadth of the temperature range from beginning to almost complete fuel conversion. This problem carries through to the CO and CO_2 profiles, which follow the too early onset of fuel conversion. A similar result was obtained in the kinetic modeling study of [10], which did not include nitromethane chemistry. In contrast, the simulation including the nitromethane sub-mechanism closely follows the experimental traces of CH_4, CO, and CO_2 with deviations that are within the experimental errors. We have investigated this strong effect of nitromethane kinetics on fuel oxidation in the presence of NO utilizing flow and sensitivity analysis.

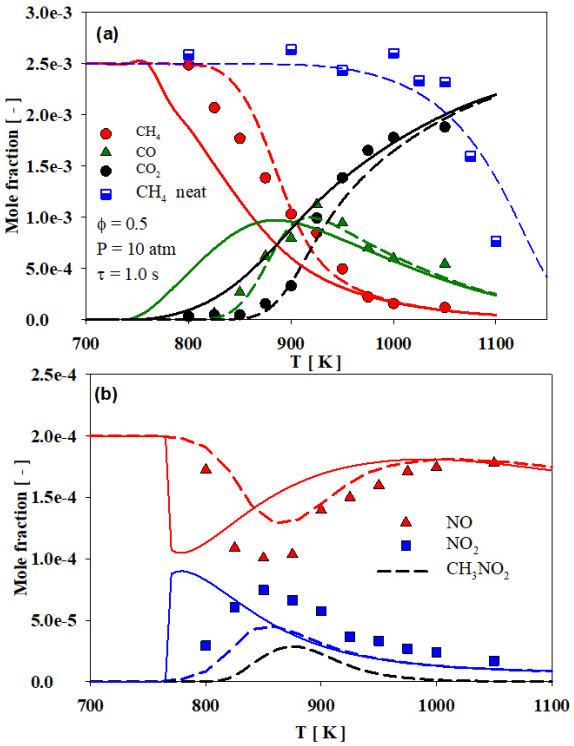

Figure 1: Oxidation of $CH_4/O_2/N_2$ doped with 200 ppm NO and without NO in JSR at 10 atm, φ = 0.5, and τ = 1.0 s. Symbols: measurements from Dagaut et al. [10], filled symbols: measurements

in the presence of NO, open symbols: measurements without NO. Solid lines: predictions without CH_3NO_2 chemistry, dashed lines: predictions with CH_3NO_2 chemistry [16].

Figure 2 shows the integrated mass flux analysis based on C-atoms (a) and based on N-atoms (b) at 840 K for the condition shown in Fig. 1 in presence of 200 ppm of NO, solid lines (without CH_3NO_2 chemistry), and dashed lines (with CH_3NO_2 chemistry). It can be observed in Figure 2(a) that CH_4 is completely decomposed to CH_3 by reacting with OH radicals in both cases. In line with the sensitivity analysis (shown in Fig. 3), it is the second most sensitive reaction. It can be observed that without CH_3NO_2 chemistry the formed CH_3 completely goes to CH_3O_2 (37 %) and CH_3O (62 %) *via* reactions CH_3O_2 (+M) =CH_3+O_2 (+M) and CH_3+NO_2=CH_3O+NO respectively. The latter reaction is the main consumption path of CH_3 radicals on the route to reactive NO radicals. The formed CH_3O_2 reacts with NO to give CH_3O and NO_2 *via* the reaction CH_3O_2+NO=CH_3O+NO_2. However, in the presence of CH_3NO_2 chemistry, the mass flux analysis (Fig. 2a) reveals that CH_3 can also combine with NO_2 to give CH_3NO_2. In line with this observation, it can be seen in Fig. 1b that the model predicts the formation of CH_3NO_2 (black dashed line) which was not measured in the experiment. The formed CH_3NO_2 readily decomposes to CH_3O + NO *via* a roaming mediated isomerization channel, a newly added path discussed in detail in our recent work [16]. It should be noted that Battin-Leclerc and co-workers [17] included CH_3NO_2 kinetics in their model (global reactions only) but they did not take into account the roaming mediated isomerization reaction path [22–25]. The importance of this path was discussed in our previous work on nitromethane degradation [16] and it turns out that it is even more important for the experiments analyzed in this study. In the absence of this channel all of the CH_3NO_2 goes to CH_2O and HONO *via* the H abstraction route (CH_3NO_2+OH=H_2O+NO+CH_2O, CH_2O+NO_2=HONO+HCO) [17], however, in our case (this study) most of the CH_3NO_2 goes to CH_3O and thus recycling back NO (see Fig. 2b). This gives rise to the reactivity retarding effect of nitromethane in the presence of NO (in Fig. 1) as revealed by the reaction path analysis shown in Fig. 2b. It can be observed that NO reacts with the radicals HO_2, CH_3O_2, OH, and CH_3O to mainly form NO_2. Without CH_3NO_2 chemistry, all of the NO_2 goes to HONO reacting with HNO, CH_3O, and the HCO radical. All the formed HONO thermally dissociates to give two reactive radicals NO and OH *via* the reaction NO+OH (+M) =HONO (+M) increasing the reactivity of the system. However, in presence of CH_3NO_2 chemistry, most of the NO_2 (62 %) reacts with CH_3 to form relatively stable CH_3NO_2 and only a minor path (35 %) goes to HONO with the just outlined reactivity enhancing effect. In line with this observation is the effect that the peak concentration of HONO is predicted a factor of 7 higher and significantly earlier when CH_3NO_2 chemistry is not present (see Fig. 4b). Vice versa, the formation of the key radicals OH and HO_2 responsible for fuel oxidation is delayed (moving towards the higher temperature) when CH_3NO_2 chemistry is present (see Fig. 4a). Hence, it can be concluded that the formation of nitromethane and its decomposition to CH_3O + NO retards the reactivity of the system in the presence of NO_x. It should be noted that NO/NO_2 interconversion also occurs *via* the reaction of NO and HO_2 radicals giving NO_2 and OH radicals and the reaction of NO_2 with H radicals reforming

NO and OH radicals. The OH radicals produced during the NO–NO_2 interchanging cycle interact with CH_4 promoting its conversion.

Furthermore, a comparison of model predictions against the recent experimental data from Song et al. [17] in the presence of NO_x (NO and NO_2) is also performed and provided in the supplementary material (Fig. S1 – S6). It is found for the NO_2 doped case (see Figure S4) that nitromethane kinetics have a similar effect as seen for the NO doped case (Figure 1). It can also be observed in Figures S1-S3 (with NO doped case) that with the increase of equivalence ratio from the lean to the rich side the effect of nitromethane kinetics on the onset of fuel oxidation is reduced significantly. This indicates that NO_x kinetics play a more important role under oxygen-rich conditions compared to the fuel-rich conditions where O_2 is consumed to form HO_2 which is subsequently converted to more reactive OH radicals [20] *via* the well-known reaction ($NO+HO_2=NO_2+OH$).

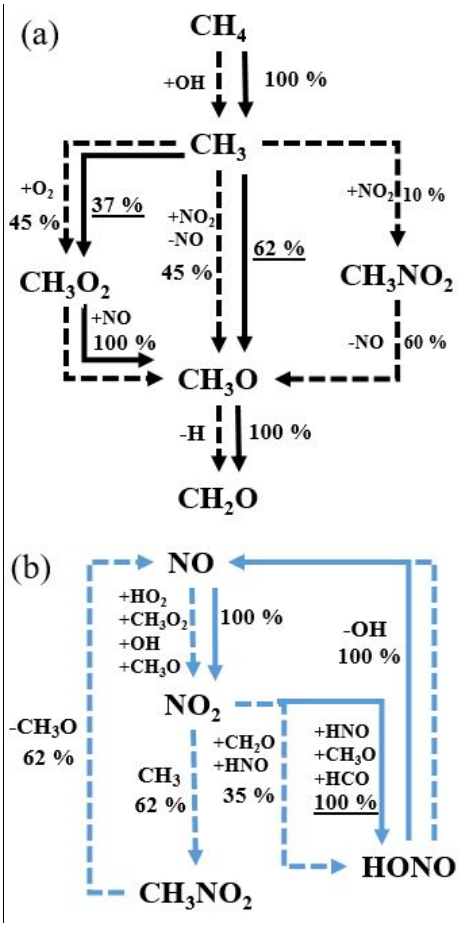

Figure 2: Reaction path analysis for the condition shown in Figure 1 (doped with NO) based on C-atom (a) based on N-atom (b) at 840 K. Solid lines: without CH_3NO_2 chemistry, dashed lines: with CH_3NO_2 chemistry.

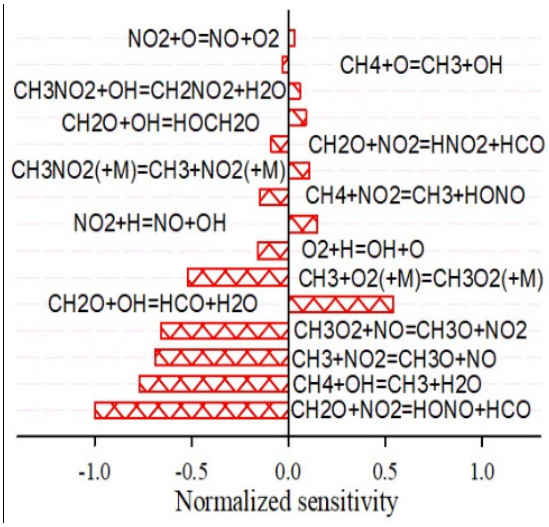

Figure 3: Normalized sensitivity analysis for the condition shown in Figure 1 (doped with NO) at 840 K towards CH_4.

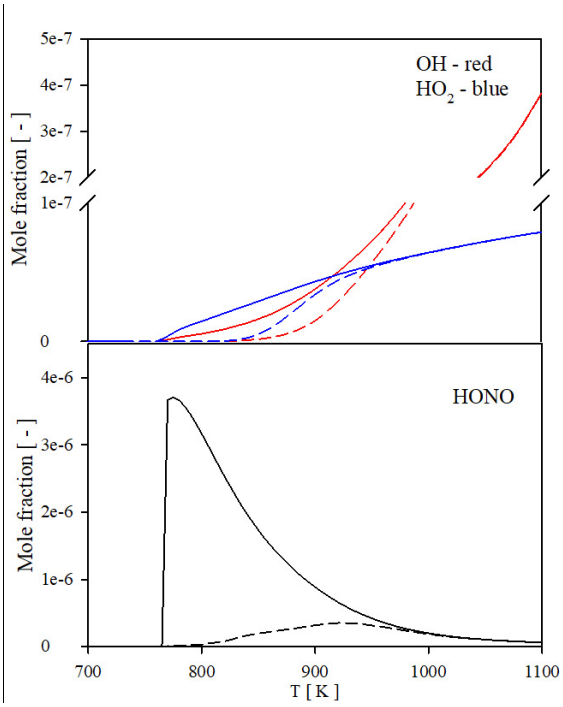

Figure 4: Predicted OH, HO_2, and HONO concentration profile with the model [16] for the condition shown in Fig. 1 (doped with NO). Dashed lines: with CH_3NO_2 chemistry; solid lines: without CH_3NO_2 chemistry.

3.2 Effect of CH_3NO_2 kinetics in *n*-heptane oxidation doped with NO

After elucidating the effect of nitromethane chemistry on CH_4 oxidation in the presence of NO, we investigate its effect on the larger hydrocarbon fuel *n*-heptane, which is a component of primary reference fuels and a simple model for the ignition of Diesel fuel.

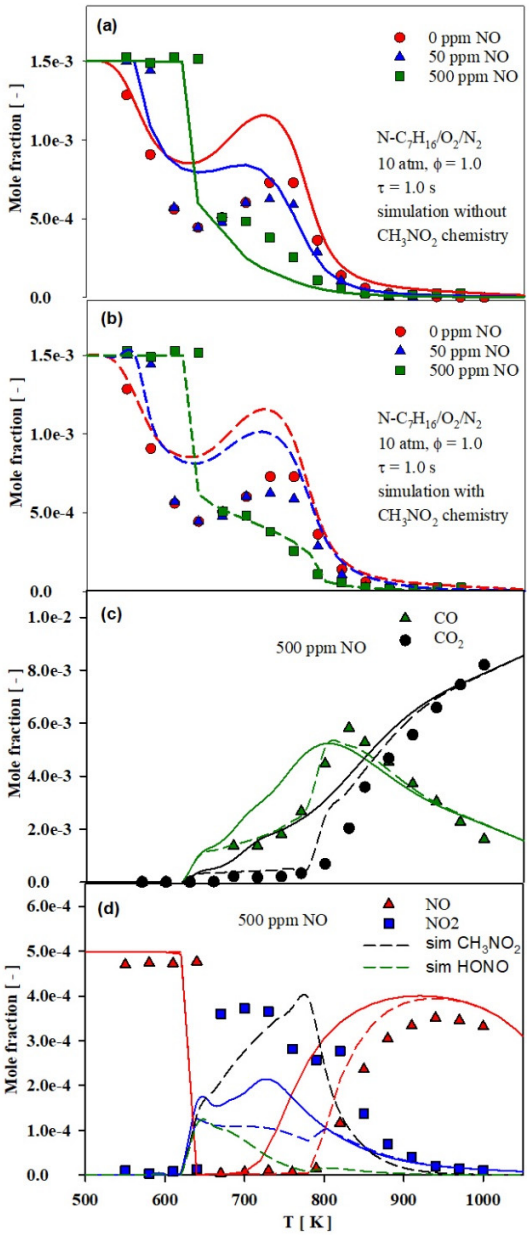

Figure 5: Oxidation of n-$C_7H_{16}/O_2/N_2$ in JSR doped with and without NO at 10 atm, φ = 1.0, τ = 1.0 s. Symbols: measurements from [12], lines: prediction with present mechanism compiled from [16,19], solid lines (without CH_3NO_2 chemistry), dashed lines (with CH_3NO_2 chemistry). N-heptane (N-C_7H_{16}) mole fraction profile (a, b); Results with 500 ppm of NO doped (c, d).

Figure 5 illustrates the oxidation of *n*-heptane (*n*-C_7H_{16}) in a JSR doped with 0, 50 and 500 ppm of NO at 10 atm and τ = 1.0 s. The experimental data are from the previous work of two of the authors of this study [11,12]. Figure 5 (a, b) shows the evolution of *n*-C_7H_{16} with temperature and Figure 5 (c, d) shows the major species profile for the case doped with 500 ppm NO. For the oxidation of neat *n*-heptane, the mole fraction - temperature dependence exhibits the well-known behavior observed for *n*-alkanes (featuring low-temperature chemistry): a first reactivity zone indicating low-temperature chemistry, a marked negative temperature coefficient area, followed by a second reactivity zone corresponding to the transition to the high-temperature chemistry. The temperature profiles of the fuel are quite different in the presence of the 50 and 500 ppm of NO. They show the ambiguous effect of NO on the oxidation of *n*-heptane: inhibition of the reaction below 650 K and a reactivity enhancement above 650 K. The temperature dependence still exhibits a negative temperature coefficient area, but it is much less pronounced than for neat *n*-heptane. This effect has been observed earlier [12,28–31], however, in all these studies the role of nitromethane chemistry in this context was not investigated. In this study, we provide such an insight on nitromethane chemistry.

It can be observed in Fig. 5a and 5b that for the neat *n*-heptane oxidation there is, as expected, no difference in *n*-C_7H_{16} prediction with and without the CH_3NO_2 chemistry, while there are significant effects when NO is present in the fuel mixture as observed in the case of methane (Fig. 1), especially for the 500 ppm NO case. We note that the model predictions do not exactly agree with the experimental measurements for neat conditions although the experimental trends are quite well reproduced. Without CH_3NO_2 chemistry the model overpredicts the effect of adding 50 ppm NO and the simulation is unable to capture the *n*-C_7H_{16} concentration profile for the 500 ppm NO case, particularly in the temperature window of 650-820 K. As in the case of methane (Fig. 1), the CH_3NO_2 chemistry has a retarding effect in this temperature range. The model also fails to predict the profiles of major species (CO, CO_2, NO, and NO_2) in this temperature window (650-820 K) when CH_3NO_2 chemistry is not included. In the presence of CH_3NO_2 chemistry, the model prediction shows good agreement with the profiles of the major species, especially with those of CO and CO_2.

Furthermore, the simulation including the nitromethane sub-mechanism also affects the predictions for intermediate species (for both 50 ppm and 500 ppm doped case), which closely follow the experimental traces in terms of peak concentration, and breadth of temperatures as shown in Fig. 6 and 7.

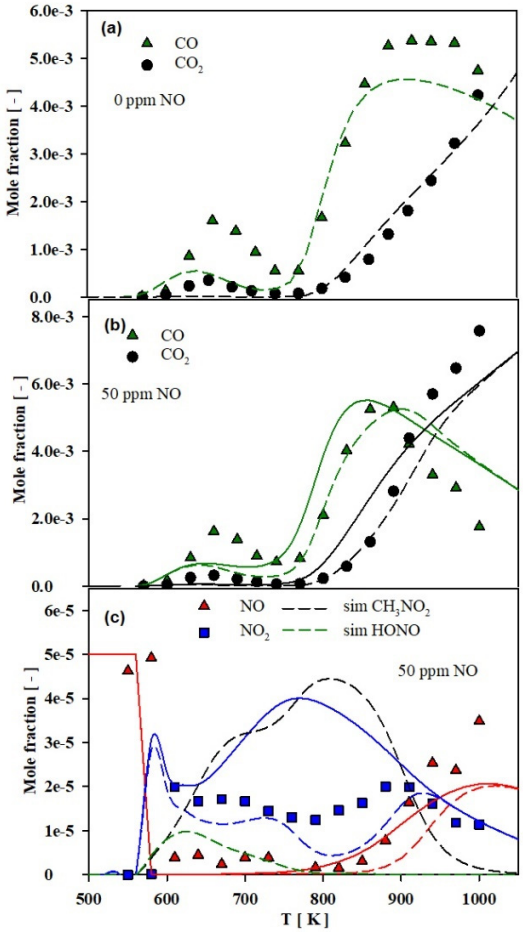

267

268 **Figure 6**: Oxidation of n-$C_7H_{16}/O_2/N_2$ in JSR doped with and without NO at 10 atm, φ = 1.0, τ = 1.0
269 s. Symbols: measurements from [12], solid lines: prediction without CH_3NO_2 chemistry, dashed
270 lines: prediction with CH_3NO_2 chemistry. Without NO in a mixture (a), with 50 ppm NO in a
271 mixture (b, c).

272

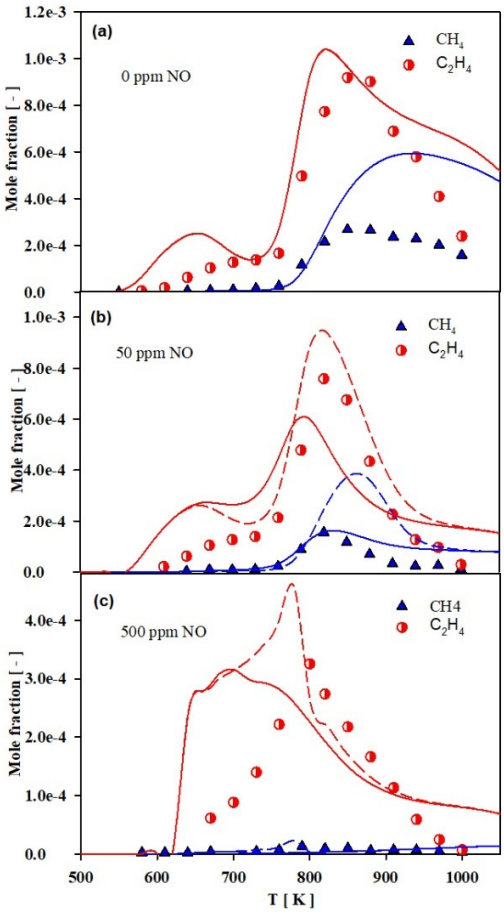

Figure 7: Oxidation of n-$C_7H_{16}/O_2/N_2$ in JSR doped with and without NO at 10 atm, φ = 1.0, τ = 1.0 s. Symbols: measurements from [11,12], solid lines: prediction without CH_3NO_2 chemistry, dashed lines: prediction with CH_3NO_2 chemistry. Without NO in a mixture (a), with 50 ppm NO in a mixture (b), with 500 ppm in a mixture (c).

An integrated mass flux analysis (based on C-atoms for 500 ppm NO doped case) at 740 K reveals (see Fig. S7 in SM) that *n*-C_7H_{16} mainly reacts to *n*-heptyl radicals *via* H atom abstraction by OH radicals. During the *n*-C_7H_{16} degradation the CH_3 radical, which is crucial for the effect of CH_3NO_2 chemistry, is formed *via* the $C_2H_5 \rightarrow C_2H_5O \rightarrow CH_3$ route. The intermediate C_2H_5 reacts with NO_2 to form C_2H_5O and NO ($C_2H_5+NO_2=C_2H_5O+NO$), the formed C_2H_5O thermally dissociates to give CH_3+CH_2O.

To elucidate the reaction pathways within the nitrogen chemistry (in 500 ppm NO doped case), we performed an integrated mass flux analysis based on N-atoms, from which the major paths are shown in Fig. 8. The analysis reveals that NO mainly reacts with HO_2 to give NO_2 in the reaction $NO+HO_2=NO_2+OH$. The minor channels that contribute to the formation of NO_2 are the direct

reaction of NO with CH_3O_2 (CH_3O_2+NO=CH_3O+NO_2), and the reverse reactions of C_2H_5+NO_2=C_2H_5O+NO, NO_2+H=NO+OH, and CH_3+NO_2=CH_3O+NO. As in the case of CH_4 (Fig. 1), NO_2 mainly goes to CH_3NO_2 (60 %) by recombining with CH_3 and 32 % of NO_2 goes to HONO reacting with HCO, CH_2O, CH_3O, *n*-C_7H_{16}, and HO_2. In line with the flow analysis, it can be seen in Figure 5d that the model predicts the formation of significant amounts of CH_3NO_2 (black dashed line). In the *n*-heptane case, CH_3NO_2 does not dissociate to CH_3O+NO *via* the roaming mediated channel but reacts *via* H atom abstraction, mainly by OH radicals, to CH_2NO_2. The change in the reaction path of CH_3NO_2 decomposition during *n*-heptane oxidation (Figure 8) is discussed below. The formed CH_2NO_2 thermally dissociates to CH_2O and NO. The formed HONO undergoes thermal decomposition to NO and OH recycling back NO and consequently producing more reactive OH radicals. In the absence of CH_3NO_2 chemistry, its formation is promoted. All of the NO_2 will go to HONO which will eventually thermally dissociate to NO and OH radicals *via* the same reaction pathways discussed above. The predicted concentration profiles of HONO are a factor of 2 higher without CH_3NO_2 chemistry (see Fig. S8 in the SM). It is clear from this analysis that for the system, in which NO is present in the mixture, CH_3NO_2 acts like a sink for the NO_2 radical, which would otherwise participate to produce more reactive OH radical accelerating the reactivity of the system (see Fig. 5a). Furthermore, the model suggests that with CH_3NO_2 chemistry the formation of the reactive radicals OH and HO_2 is delayed (moving towards higher temperature, see Fig. S8 in the SM), the same as seen for the methane case above (Fig. 4). The effect of CH_3NO_2 chemistry on the overall reactivity is significant as can be seen in the sensitivity analysis (Fig. 9) which identifies the recombination reaction CH_3NO_2(+M)=CH_3+NO_2(+M) among the most sensitive reactions at 740 K.

As stated above we observed a change in the reaction path of CH_3NO_2 decomposition during *n*-heptane oxidation (Figure 8) compared to the CH_4 oxidation (Figure 2). The CH_3NO_2 decomposition is mainly controlled by OH and HO_2 formation. In the case of *n*-heptane oxidation HO_2 begins to form at a much lower temperature compared to CH_4 (see Figure S10 in SM). The higher amount of HO_2 formation at a lower temperature is due to the low temperature chemistry (NTC regime) of *n*-heptane (the model reveals that many oxygenated species from *n*-heptane chemistry contributes to HO_2 formation). However, CH_4 does exhibit low temperature chemistry (NTC regime) and HO_2 formation is negligible compared to the *n*-heptane case (see Figure S10 in SM). It is also interesting to observe that the formation of HO_2 and CH_3NO_2 begins at the same temperature in the case of *n*-heptane oxidation. The early formation of HO_2 radicals in the case of *n*-heptane oxidation supports the early formation of OH radical via route NO+HO_2=NO_2+OH (80% of formed HO_2 is consumed to form OH). The formed OH radical reacts with CH_3NO_2 via the H-abstraction channel to give CH_2NO_2. In the case of CH_4 oxidation there is a lack of OH radicals in the system at a lower temperature (see Figure S10 in SM). Furthermore, in the case of CH_4 oxidation (see Figure S10 in SM) at 900 K we observe the OH formation in the system. Indeed, at this temperature model reveals that CH_3NO_2 reacts with OH radical to form CH_2NO_2

(CH_3NO_2+OH=CH_2NO_2+H_2O) and eventually leading to CH_2O+NO via thermal dissociation of CH_2NO_2 (see Figure S11 in SM). This analysis leads to the conclusion that the decomposition path of CH_3NO_2 is mainly controlled by the radical pool in the system which can vary depending upon fuel and the system operating condition.

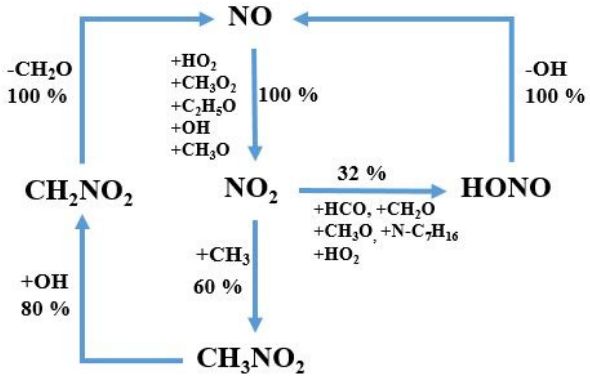

Figure 8: Reaction path analysis based on N-atoms for the conditions shown in Figure 5 (here 500 ppm of NO) at 740 K with CH_3NO_2 chemistry.

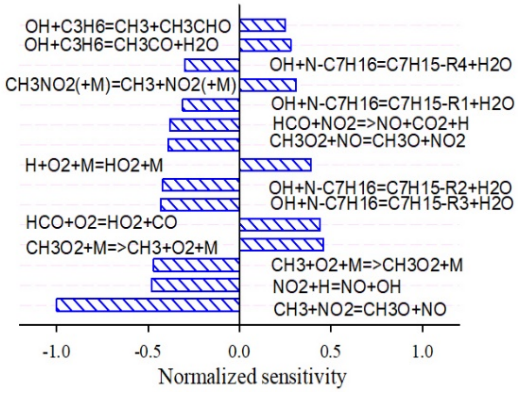

Figure 9: Normalized sensitivity analysis for the conditions shown in Figure 5 (500 ppm of NO) at 740 K towards *n*-C_7H_{16}.

Figure 10 illustrates the predicted mole fractions of the key intermediates HONO and CH_3NO_2 during *n*-C_7H_{16}/O_2/N_2 oxidation in a JSR doped with 500 ppm of NO at 1 (solid lines) and 10 atm (dashed lines) respectively. It can be observed that a pressure increase from 1 to 10 atm, increases HONO and CH_3NO_2 concentrations by factors ~6 and 5 respectively. The stabilization of CH_3NO_2 at higher pressures supports HONO formation *via* CH_3NO_2 and reflects the pressure dependent CH_3NO_2 (+M) =CH_3+NO_2 (+M) reaction. It should be noted that all the attempts to detect these two species in previous experimental studies [17,18] were carried out near 1 atm pressure. The findings of this work strongly suggest a high importance of CH_3NO_2 chemistry for

the ignition timing of *n*-heptane at elevated pressure (and engine relevant conditions), for which an experimental detection of CH_3NO_2 and HONO may be possible.

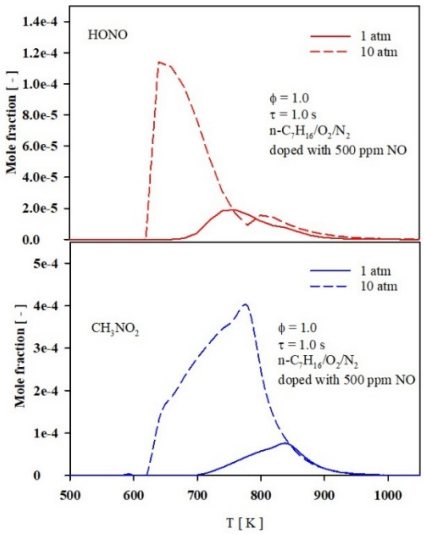

Figure 10: Model predicted concentration profile comparison for HONO and CH_3NO_2 with CH_3NO_2 chemistry during oxidation of n-$C_7H_{16}/O_2/N_2$ in JSR doped with 500 ppm of NO, φ = 1.0, τ = 1.0 s (a condition similar to Fig. 5). Solid lines: 1 atm, dashed lines: 10 atm.

4. Conclusion

A detailed investigation of the CH_3NO_2 chemistry effect on fuel-NO interactions has been performed for the fuels methane and *n*-heptane using a recently developed and extensively validated $H_2/O_2/CO/NO_x/NH_3/CH_3NO_2$ baseline chemistry. We found that CH_3NO_2 kinetics retard the system reactivity in the low temperature range by delaying the production of key radicals like OH and HO_2. This chemistry is crucial to understand and adequately simulate the delicate NO effect on the ignition timing of *n*-heptane/NO mixtures, namely the transition from retardation to reactivity enhancement at temperatures around 650 K. Further, the model suggests that CH_3NO_2 is the major source of NO_2 consumption decreasing the concentration of HONO, which is also formed *via* competing reactions of NO_2. For both fuels, HONO was found to contribute significantly to the formation of OH and the recycling of NO. For *n*-heptane, the model suggests that at higher pressure, relevant to engine condition, the two key intermediate species HONO and CH_3NO_2 feature strongly increased concentrations and they may be detectable under high-pressure conditions in combustion experiments of this fuel-NO_x system. The results of this work call for detailed future investigations of the CH_3NO_2 chemistry effect in the context of exhaust gas recirculation, also with regard to the suppression of engine knock. Clearly, the chemistry of this key intermediate imposes important kinetic constraints for simulating the specific low-temperature oxidation of fuel – NO_x systems.

References

[1] P.J. Crutzen, The role of NO and NO2 in the chemistry of the troposphere and stratosphere., Annu. Rev. Earth Planet. Sci. Vol. 7. 7 (1979) 443–472. doi:10.1146/annurev.ea.07.050179.002303.

[2] K. Hoyermann, F. Mauss, M. Olzmann, O. Welz, T. Zeuch, Exploring the chemical kinetics of partially oxidized intermediates by combining experiments, theory, and kinetic modeling, Phys. Chem. Chem. Phys. 19 (2017) 18128–18146. doi:10.1039/C7CP02759A.

[3] O. Welz, J.D. Savee, D.L. Osborn, S.S. Vasu, C.J. Percival, D.E. Shallcross, C.A. Taatjes, Direct kinetic measurements of Criegee intermediate (CH_2OO) formed by reaction of CH_2I with O_2., Science. 335 (2012) 204–7. doi:10.1126/science.1213229.

[4] L.V. Moskaleva, M.C. Lin, The spin-conserved reaction CH+N2→H+NCN: A major pathway to prompt no studied by quantum/statistical theory calculations and kinetic modeling of rate constant, Proc. Combust. Inst. 28 (2000) 2393–2401. doi:10.1016/S0082-0784(00)80652-9.

[5] W. Hack, M. Hold, K. Hoyermann, J. Wehmeyer, T. Zeuch, Mechanism and rate of the reaction CH3+ O - Revisited, Phys. Chem. Chem. Phys. 7 (2005) 1977–1984. doi:10.1039/b419137d.

[6] E. Goos, C. Sickfeld, F. Mauss, L. Seidel, B. Ruscic, A. Burcat, T. Zeuch, Prompt NO formation in flames: The influence of NCN thermochemistry, Proc. Combust. Inst. 34 (2013) 657–666. doi:10.1016/j.proci.2012.06.128.

[7] J.M. Anderlohr, R. Bounaceur, A. Pires Da Cruz, F. Battin-Leclerc, Modeling of autoignition and NO sensitization for the oxidation of IC engine surrogate fuels, Combust. Flame. 156 (2009) 505–521. doi:10.1016/j.combustflame.2008.09.009.

[8] M. Sarabi, E. Abdi Aghdam, Experimental analysis of in-cylinder combustion characteristics and exhaust gas emissions of gasoline–natural gas dual-fuel combinations in a SI engine, J. Therm. Anal. Calorim. (2019) 1–14. doi:10.1007/s10973-019-08727-2.

[9] S.K. Prabhu, H. Li, D.L. Miller, N.P. Cernansky, The effect of nitric oxide on autoignition of a primary reference fuel blend in a motored engine, in: SAE Tech. Pap. 932757, 1993. doi:10.4271/932757.

[10] P. Dagaut, A. Nicolle, Experimental study and detailed kinetic modeling of the effect of exhaust gas on fuel combustion: Mutual sensitization of the oxidation of nitric oxide and methane over extended temperature and pressure ranges, Combust. Flame. 140 (2005) 161–171. doi:10.1016/j.combustflame.2004.11.003.

[11] G. Moréac, Experimental study and modelling of chemical interactions between gases residual and fresh gas in the homogeneous spontaneous ignition gasoline engines, PhD Thesis, University of Orléans, 2003. https://tel.archives-ouvertes.fr/tel-02961685/.

[12] G. Moréac, P. Dagaut, J.F. Roesler, M. Cathonnet, Nitric oxide interactions with hydrocarbon oxidation in a jet-stirred reactor at 10 atm, Combust. Flame. 145 (2006) 512–520. doi:10.1016/j.combustflame.2006.01.002.

[13] R. Lan, J.T.S. Irvine, S. Tao, Ammonia and related chemicals as potential indirect hydrogen storage materials, Int. J. Hydrogen Energy. 37 (2012) 1482–1494. doi:10.1016/j.ijhydene.2011.10.004.

[14] K.P. Shrestha, L. Seidel, T. Zeuch, F. Mauss, Detailed Kinetic Mechanism for the Oxidation of Ammonia Including the Formation and Reduction of Nitrogen Oxides, Energy & Fuels. 32 (2018) 10202−10217. doi:10.1021/acs.energyfuels.8b01056.

[15] K.P. Shrestha, L. Seidel, T. Zeuch, F. Mauss, Kinetic Modeling of NOx Formation and Consumption during Methanol and Ethanol Oxidation, Combust. Sci. Technol. 191 (2019) 1628–1660. doi:10.1080/00102202.2019.1606804.

[16] K.P. Shrestha, N. Vin, O. Herbinet, L. Seidel, F. Battin-Leclerc, T. Zeuch, F. Mauss, Insights into nitromethane combustion from detailed kinetic modeling – Pyrolysis experiments in jet-stirred and flow reactors, Fuel. 261 (2020) 116349. doi:10.1016/j.fuel.2019.116349.

[17] Y. Song, L. Marrodán, N. Vin, O. Herbinet, E. Assaf, C. Fittschen, A. Stagni, T. Faravelli, M.U. Alzueta, F. Battin-Leclerc, The sensitizing effects of NO 2 and NO on methane low temperature oxidation in a jet stirred reactor, Proc. Combust. Inst. 37 (2019) 667–675. doi:10.1016/j.proci.2018.06.115.

[18] L. Marrodán, Y. Song, O. Herbinet, M.U. Alzueta, C. Fittschen, Y. Ju, F. Battin-Leclerc, First detection of a key intermediate in the oxidation of fuel + NO systems: HONO, Chem. Phys. Lett. 719 (2019) 22–26. doi:10.1016/j.cplett.2019.01.038.

[19] L. Seidel, K. Moshammer, X. Wang, T. Zeuch, K. Kohse-Höinghaus, F. Mauss, Comprehensive kinetic modeling and experimental study of a fuel-rich, premixed n-heptane flame, Combust. Flame. 162 (2015) 2045–2058. doi:10.1016/j.combustflame.2015.01.002.

[20] K.P. Shrestha, S. Eckart, A.M. Elbaz, B.R. Giri, C. Fritsche, L. Seidel, W.L. Roberts, H. Krause, F. Mauss, A comprehensive kinetic model for dimethyl ether and dimethoxymethane oxidation and NOx interaction utilizing experimental laminar flame speed measurements at elevated pressure and temperature, Combust. Flame. 218 (2020) 57–74. doi:10.1016/j.combustflame.2020.04.016.

436 [21] R.S. Zhu, M.C. Lin, CH3NO2 decomposition/isomerization mechanism and product
437 branching ratios: An ab initio chemical kinetic study, Chem. Phys. Lett. 478 (2009) 11–16.
438 doi:10.1016/J.CPLETT.2009.07.034.

439 [22] Z. Homayoon, J.M. Bowman, Quasiclassical trajectory study of CH3NO2 decomposition
440 via roaming mediated isomerization using a global potential energy surface, J. Phys.
441 Chem. A. 117 (2013) 11665–11672. doi:10.1021/jp312076z.

442 [23] R.S. Zhu, P. Raghunath, M.C. Lin, Effect of roaming transition states upon product
443 branching in the thermal decomposition of CH3NO2, J. Phys. Chem. A. 117 (2013) 7308–
444 7313. doi:10.1021/jp401148q.

445 [24] C.J. Annesley, J.B. Randazzo, S.J. Klippenstein, L.B. Harding, A.W. Jasper, Y. Georgievskii,
446 B. Ruscic, R.S. Tranter, Thermal Dissociation and Roaming Isomerization of
447 Nitromethane: Experiment and Theory, J. Phys. Chem. A. 119 (2015) 7872–7893.
448 doi:10.1021/acs.jpca.5b01563.

449 [25] A. Matsugi, H. Shiina, Thermal Decomposition of Nitromethane and Reaction between
450 CH3 and NO2, J. Phys. Chem. A. 121 (2017) 4218–4224. doi:10.1021/acs.jpca.7b03715.

451 [26] P.A. Vlasov, N.M. Kuznetsov, Y.P. Petrov, S. V. Turetskii, Nitromethane Isomerization
452 during Its Thermal Decay, Kinet. Catal. 59 (2018) 6–10.
453 doi:10.1134/S0023158418010147.

454 [27] http://logesoft.com/loge-software/, (n.d.).

455 [28] H. Zhao, L. Wu, C. Patrick, Z. Zhang, Y. Rezgui, X. Yang, G. Wysocki, Y. Ju, Studies of low
456 temperature oxidation of n-pentane with nitric oxide addition in a jet stirred reactor,
457 Combust. Flame. 197 (2018) 78–87. doi:10.1016/j.combustflame.2018.07.014.

458 [29] Z. Chen, P. Zhang, Y. Yang, M.J. Brear, X. He, Z. Wang, Impact of nitric oxide (NO) on n-
459 heptane autoignition in a rapid compression machine, Combust. Flame. 186 (2017) 94–
460 104. doi:10.1016/j.combustflame.2017.07.036.

461 [30] P.A. Glaude, N. Marinov, Y. Koshiishi, N. Matsunaga, M. Hori, Kinetic modeling of the
462 mutual oxidation of NO and larger alkanes at low temperature, Energy and Fuels. 19
463 (2005) 1839–1849. doi:10.1021/ef050047b.

464 [31] A. Dubreuil, F. Foucher, C. Mounaïm-Rousselle, G. Dayma, P. Dagaut, HCCI combustion:
465 Effect of NO in EGR, Proc. Combust. Inst. 31 II (2007) 2879–2886.
466 doi:10.1016/j.proci.2006.07.168.

467